Full Paper

Electrochemical Synthesis and Characterization of 1,2-Naphthaquinone-4-Sulfonic Acid Doped Polypyrrole

Richard Odunayo Akinyeye,[a] *Immaculate Michira,*[a] *Mantoa Sekota,*[a] *Amir Al Ahmed,*[a] *Duarte Tito,*[c]
Priscilla Gloria Lorraine Baker,[a]* *Christopher Michael Ashton Brett,*[b] *Maher Kalaji,*[c] *Emmanuel Iwuoha*[a]*

[a] Sensor Research Laboratory, Department of Chemistry, University of the Western Cape, Bellville 7535, South Africa
*e-mail eiwuoha@uwc.ac.za; pbaker@uwc.ac.za
[b] Department de Quinica, Universidade de Coimbra, 3004-535 Coimbra, Portugal
[c] School of Chemistry, University of Wales, Bangor LL572UW, UK

Abstract
Polypyrrole thin film microelectrodes prepared from an aqueous solution of the sodium salt of 1, 2-napthaquinone-4-sulfonic acid and pyrrole in hydrochloric acid as the supporting electrolyte was characterized electrochemically for the first time and found to exhibit good electronic and spectroscopic properties. Voltammetric investigations showed that the polymer exhibited quasireversible kinetics in a potential window of -400 mV to 700 mV, with a formal potential of 322 mV vs. Ag/AgCl. The diffusion coefficient was calculated to be 1.02×10^{-6} cm^2 s^{-1} for a thin film with a surface concentration of 1.83×10^{-7} mol cm^{-2} having a rate constant of 2.20×10^{-3} cm s^{-1} at 5 mV s^{-1}. Electrochemical impedance spectroscopy provided quantitative information about the conductivity changes within the modified polymer and support for the quasireversible kinetics suggested by voltammetry. The changes in electrical properties of the polymer during electrochemical p-doping and n-doping were quantified by equivalent electrical circuit fitting and assisted in the identification of the suggested kinetic mechanism. SNIFTIRS confirmed the incorporation of the surfactant into the polypyrrole film and for the first time structural changes within the polymer were observed that could be related to the observed electrochemistry of the polymer.

Keywords: Polypyrrole, 1,2-Napthaquinone-4-sulfonic acid, Electropolymerization, Impedance spectroscopy, Conductivity, SNIFTIRS

1. Introduction

Polypyrrole (PPy) is an intrinsically conducting polymer with various interesting properties [1, 2]. Its synthesis, characterization, and applications have received a lot of attention in publication over the past two decades but there is still a challenge in the control of synthesis conditions and the nature of dopant ion introduced in order to generate new sensor materials with favorable electrochemistry, morphology, and spectroscopic properties [3–14]. By employing chemical synthesis routes the polypyrrole is mainly produced in the bulk solution and the transfer of the polypyrrole to a suitable electrode surface is limited. Polypyrrole is insoluble in most common solvents and adherence of polypyrrole to the electrode surface during sensor preparation, is also problematic in the absence of suitable dopants that improves its properties. These disadvantages however may be avoided, if electrochemical polymerization is applied [15–21]. Thickness and morphology of the film are easily controlled by type of solvent, electrolyte concentration and type of electrode material, current density, applied potential, polymerization time and temperature [15, 16]. The optimization of these parameters in order to obtain nanostructured and reasonably stable PPy in air and in aqueous media opens the way for entrapment and/or doping of polypyrrole by various biomaterials such as small organic molecules, DNA, proteins and even living cells [17–20]. In particular cases, PPy may be synthesized in the overoxidized state and entrapped molecules may be removed to produce molecularly imprinted polymer electrodes. Electropolymerization also allows the deposition of films independent of the electrochemical cell geometry and this is particularly useful in the design of micro fluidic systems [21].

Surfactants are used as polymer additives in order to control the morphology and when implicitly incorporated into the conducting polymer backbone, it serves to improve the conductivity, stability, solubility in organic solvents and processability [22]. Surfactants affect the preparation of conducting polymers in three ways, i.e., (i) the micelles control the distribution of reactants between the micellar and the aqueous phase and thus exerts some control over the polymerization pathway (ii) anionic surfactants may act as counter ions for the polymer polycations and (iii) the hydrophobic tail of the surfactant may adsorb on the polymer formed at the electrode surface and thus becomes part of the resulting material, influencing its chemical properties [23].

We have recently prepared 1, 2-naphthaquinone sulfonic acid doped polypyrrole (PPyNQSA) through potentiodynamic electropolymerization from aqueous solution, at low pH on a platinum disk electrode to form stable thin films with good electrochemical activity, improved conductivity and visibly different colors on the oxidized state as opposed to the neutral state. By subjecting these films generated in situ, to intensive electrochemical characterization we propose a mechanism to support the unique electrochemistry of the doped polypyrrole films. This paper reports our spectro- and electrochemical investigation on the electrosynthesized film, which showed improved properties. These improved properties of the modified polymer material lend itself favorably to applications in fuel cells, chemical sensors, controlled drug delivery, switching based on electrochromic control, corrosion protection, and environmental remediation.

2. Experimental

2.1. Chemicals

The Pyrrole (98%) used was supplied by Sigma-Aldrich (Pty) Ltd., South Africa. This was distilled at reduced pressure, saturated with argon gas, and kept in 1-cm^3 ampoules in the dark at 4 °C. The sodium salt of 1, 2-naphthaquinone-4-sulfonic acid (BDH laboratory reagent) was used as the dopant. The electrolyte used in the polymerization and all electrochemical characterization experiments was prepared from hydrochloric acid (32%) (Fluka) and distilled water (specific resistance 18 MΩ, Milli-Q, Millipore).

2.2. Voltammetric Measurements

Cyclic voltammetric (CV), Osteryoung square wave voltammetry (OSWV) and differential pulse voltammetry (DPV) measurements were made using a BAS 50W integrated automated electrochemical workstation (Bioanalytical Systems, Lafayate, IN, USA). The three electrode cell used contained a platinum disk electrode with a surface area of 0.0201 cm^2 as working electrode which was polished to a shiny finish using slurries of 0.3 μm and 0.05 μm fine alumina powders (Bueller, IL, USA), and rinsed with deionized water. The reference electrode used was Ag/AgCl electrode -BAS MF-2052 (3 M NaCl type) and the counter electrode was a polished platinum wire. The electrolyte used in all the electrochemical experiments, was HCl. A thin film of conducting polypyrrole was grown under potentiodynamic conditions from a solution containing the 350-μL pyrrole monomer (0.0050 moles) and 0.130 g of the sodium salt of 1, 2-naphthaquinone-4-sulfonic acid-dopant (0.0005 moles) respectively in 50 mL of 0.05 M HCl. The solution from which the film was generated was then replaced with a fresh electrolyte solution of 0.05 M HCl, in which all cyclic voltammetry experiments were then per-

formed. The potential window used for the polymerization and characterization studies was −400 mV to 700 mV vs. Ag/AgCl. OSWV were performed at 5 Hz at 25 mV square wave amplitude using a potential step of 4 mV from an initial potential, E_i, of −400 mV to a final potential, E_f, of 700 mV. DPV experiments were performed at scan rates of 5, 10 and 20 mV at pulse amplitude of 25 mV.

2.3. EIS Measurements

EIS measurements were performed on the thin film of NQSA-doped polypyrrole from 2.2 using a PGZ402 Voltalab Analyzer (Radiometer Analytical S.A, France) and the same three-electrode cell arrangement and electrolyte as for cyclic voltammetry. An AC amplitude of 10 mV at different applied potentials between 0 and 600 mV at 50 mV intervals, over a frequency range from 10^5 to 10^{-2} Hz in 20 steps per frequency decade. Data analysis was done by modeling with equivalent electrical circuits using Z-View software.

2.4. SNIFTIRS

Subtractively normalized interfacial Fourier transform infrared spectroscopy (SNIFTIRS) measurements were performed in the staircase mode using a fully evacuated FTIR spectrometer (Bruker IFS113v) fitted with a mercury cadmium telluride (MCT) photo detector and Ge/KBr beam splitter. The thin film of polypyrrole generated as in 2.2 above was subjected to SNIFTIRS analysis using a custom built thin-layer three-electrode cell. The reflectance data on the film at the working electrode was collected at different applied potential using a manually controlled potentiostat. A calomel reference electrode was used and a platinum ring electrode fitted on the inside of the custom made FTIR electrochemical cell, served as counter electrode [24]. During the in situ measurements of FTIR spectra the surface of the working electrode was positioned very close to the CaF$_2$ window and parallel to it in order to limit the influence of solvent on the spectra. Spectra were obtained at potentials from 0 mV to 600 mV at 100 mV intervals. Spectra were also recorded at selected potentials in the reverse direction as a check on the reversibility of the modified polymer. Spectra were obtained by Fourier transformation after averaging 200 interferograms acquired at each potential, using p-polarized radiation. Infrared spectra have been normalized with respect to the reference spectrum collected at 0 mV and are displayed as $\Delta R/R$ difference spectra (the ratio of the signals obtained at potentials E_i and E_{ref} and that obtained at the reference potential E_{ref}) in units of reflectance, since no logarithm was applied [25].

Subtractively normalized SNIFTIRS spectra obtained in this way therefore, contain only information of the molecular changes occurring from modification of the oxidation state of the polymer. Negative bands were interpreted as indicative of absorption by species generated as the

potential is changed to E_i, while upward peaks were interpreted as the disappearance of initial species [26].

3. Results and Discussion

3.1. Voltammetry

The potentiodynamic behavior of the modified polypyrrole is shown in Figure 1. The electrochemically-polymerized film, grown at a scan rate of 50 mV s^{-1} for 25 cycles, was observed to have good adhesion to the Pt electrode surface. It should be noted that the ratio of the mole concentration of the monomer/dopant mixture is critical in order to produce a conducting polymer. A potential window of -400 through 700 mV vs. Ag/AgCl was used for the polymerization and investigation after optimization of the synthesis conditions. This optimum range was arrived at based on the over-oxidation and degradation of polypyrrole at higher positive potentials, whilst a too negative potential will result in hydrogen evolution [27]. The cyclic voltammograms consistently displayed one distinctive oxidation and one reduction peak. The peak separation between the anodic and cathodic peaks, increased with increase in scan rates. From our multiscan rate voltammograms (Fig. 1), the anodic/cathodic peak potentials were 364 mV and 301 mV vs. Ag/AgCl respectively at 5 mV s^{-1}. The average formal potential ($E^{\circ\prime}$) estimated from peak potentials at 5, 10, 15, 25, 30, 40 and 50 mV s^{-1} was calculated as 322 ± 5 mV. DPV investigation at a scan rate of 5 mV s^{-1} gave both anodic and cathodic peaks at 317 mV while the OSWV at a frequency of 15 Hz and amplitude of 25 mV gave a formal potential ($E^{\circ\prime}$) value of 317 mV. The CV peak separation of 63 mV at 5 mV s^{-1} was used as an indication of a one electron process for the polymer.

The Brown Anson equation, $\{I_p = n^2 F^2 \Gamma^*_{PPyNQSA}.Av/4RT\}$, was used to estimate the surface concentration of the polymer ($\Gamma^*_{PPyNQSA}$) using the peak currents (I_p) obtained at different scan rates (v) between 5 mV s^{-1} and 50 mV s^{-1} [28].

The notations F, A, R and T are constants for the Faraday's constant (96584 C mol^{-1}), working electrode area, molar gas constant and room temperature of 298 K respectively. The plots gave a trend that confirms the formation of a stable film whose density is slightly lower during reduction (1.42 $\times$ 10^{-7} mol $\cdot$ cm^{-2}) as compared to oxidation (1.83 $\times$ 10^{-7} mol $\cdot$ cm^{-2}). The plots showed linear relationship with correlation coefficient (r^2) of 0.999 and 0.994 respectively for the anodic and cathodic currents vs. scan rates. The ratio of anodic peak current ($I_{p,a}$) to cathodic peak current ($I_{p,c}$) ranged from 1.23 to 1.38 over the range of scan rates applied, which is not exactly unity as required for fully reversible one electron transfer, and therefore a quasireversible electron transfer mechanism is suggested.

The systems displayed progressive shift in anodic peak potential towards more positive values coupled with shift in cathodic peak potential to less positive values with increase in scan rate. The separations increase progressively from 63 mV at 5 mV s^{-1} to 166 mV at 50 mV s^{-1} coupled with increase in the magnitude of the peak currents with increase in scan rates. This shows that the peak currents are diffusion controlled. Thus the Randel–Sevcik equation $\{I_p/v^{1/2} = 2.686 \times 10^5 n^{3/2} A \Gamma^*_{PPyNQSA} D_e^{1/2}\}$ was applied to determine the diffusion coefficient (D_e) for electron hopping along the polymer chain [29]. I_p is the peak current in A, n is the number of electron transferred, v is the scan rate in V s^{-1}, n is the no of electrons transferred, A is the surface area of the electrode cm^2, $\Gamma^*_{PPyNQSA}$ is the surface concentration of the polymer film in mol cm^2, D_e, is the rate a charge transportation in cm^2 s^{-1} along the polymer chain. The slopes of the linear plots are 1.0309 and 0.8025 A/(V/s)$^{1/2}$ for the oxidation and reduction scan waves with a corresponding correlation coefficient of 0.981 and 0.991 respectively. D_e, indicating the rate of electron transfer along the polymer chain, was found to be the same for the oxidation and reduction reaction, i.e., 1.02 $\times$ 10^{-6} cm^2 s^{-1}. This suggests that the deviation from full reversibility does not necessarily involve permanent electronic changes to the bulk polypyrrole film upon potential cycling, but that some other phenomenon is responsible for the kinetics observed.

The cyclic voltammogram at a scan rate of 5 mV s^{-1} was used to investigate the rate constant (k^0) for electron transfer within the polymer chain using Nicholson treatment for a quasireversible electrochemical system using the equation $\{k^0 = \varphi (\alpha n F v D_e/RT)^{1/2}\}$ [29–31].

The diffusion coefficient (D_e) is in cm^2 s^{-1}; molar gas constant (R) is in J mol^{-1} K^{-1}; Faraday's constant (F) in C and temperature (T) being in K. The transfer coefficient, α, of 0.5 was assumed for the PPyNQSA systems and the kinetic parameter, φ (dimensionless), was assigned a value of 7 based on the peak separation, ΔE_p, of 63 mV at a scan rate of 5 mV s^{-1} which indicated $n = 1.1$. The k^0 value of 2.20 $\times$ 10^{-3} cm s^{-1} obtained for the polymer at 5 mV s^{-1} shows that electron hopping along the polymer chain at the low scan rate is quite facile. This is comparable with the rate constants reported for other conducting polymers vis. Pt/polyaniline electrodes with k^0 values of 0.049 to 5.4 $\times$ 10^{-3} cm s^{-1} in different electrolytes [32] and Pt/ poly(3,4-ethyl-
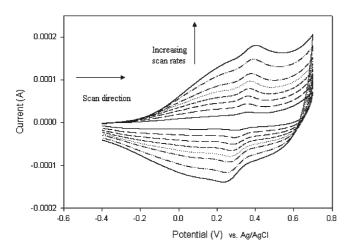

Fig. 1. Multiscan rate voltammograms obtained at a modified platinum electrode with a thin film of PPyNQSA in 0.05 M HCl at scan rates of 5, 10, 15, 20, 25, 30, 40, and 50 mV s^{-1}.

enedioxythiophene) electrodes with k^0 values of 1.5 to 45.3×10^{-3} cm s^{-1} when prepared under different synthesis conditions [33].

3.2. Impedance Spectroscopy

Electrochemical impedance spectroscopy (EIS) enables the separation of interfacial electron transfer from concomitant electronic changes occurring within the bulk material of the electrode on the basis of frequency dependent electrochemical response. EIS data was collected, in consecutive 50 mV steps, in the potential range corresponding to the oxidation of the polymer film (0 mV to 600 mV) and the subsequent reduction by inversion of the steps in potential back to 0 mV.

Typical data obtained at an applied potential of $+50$ mV vs. Ag/AgCl are shown in the complex plane impedance plots of Figure 2. The data obtained was analyzed using an equivalent electrical circuit consisting of the solution resistance (R_s), an R_1CPE_1 parallel combination, where CPE is a constant phase element, to model movement by electron hopping through the polymer film along the polymer backbone, and a second R_2C_2 component in series representing the electrode /solution interface, as indicated in [34, 35]. The CPE was modeled as a nonideal capacitance, according to

$$CPE = 1/(Ci\omega)^n$$

The *CPE* is defined by two values, i.e., the capacitance, *C*, and the *CPE* exponent, *n*, which has a value between 0.5 and

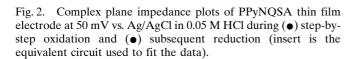1 for a nonideal capacitor. If *n* equals 1, the equation is identical to that of a capacitor and smaller values can be related to surface roughness and inhomogeneities, which lead to frequency dispersion. When a *CPE* is placed in parallel to a resistor, a depressed semicircle (Cole-element) is produced. The solution resistance varied from 9.6 to 11.0 Ω. The values of R_1 and CPE_1 were interpreted through the electrical characteristics of the electropolymerized PPyNQSA polymer bulk material. The capacitive nature of the bulk material was substantiated by the inverse relationship between the capacitance and resistance values of the high frequency loop. The polymer material showed good conductivity (10–20 Ω) and in the region of the formal potential as obtained by voltammetric experiments, the conductivity of the polymer material was measured as 10.8 Ω. The average value of *n* for all experiments was 0.56, which is indicative of a rather rough morphology and porous structure and is probably also associated with electron hopping along the polymer backbone. The interface of the polymer with the HCl electrolyte showed consistently low values of capacitance, C_2 (30 μF) and resistance, R_2 (2.7–4.2 Ω) during the oxidation steps, the latter reaching a minimum value of 2.7 Ω at the formal oxidation potential. The electron transfer from solution to the polymer film during oxidation is thought to be direct electron transfer without mediation by any surface bound species, since the interfacial capacitance values of 16 μF hardly varied over the potential range studied.

During the subsequent reduction steps, from 600 mV to 0 mV vs. Ag/AgCl, the capacitance (2 mF) and the resistance (15.5 Ω) of the polymer bulk material remained fairly constant. The bulk capacitance (CPE_1) and resistance (R_1) values were of the same order of magnitude during the reduction steps as compared with oxidation. However, a plot of the interfacial capacitance (C_2) versus applied potential showed a gradual increase in capacitance as the potential became more negative, and gradual increase as it became more positive (Fig. 3). The capacitance values for
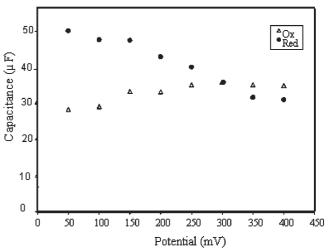
Fig. 2. Complex plane impedance plots of PPyNQSA thin film electrode at 50 mV vs. Ag/AgCl in 0.05 M HCl during (●) step-by-step oxidation and (●) subsequent reduction (insert is the equivalent circuit used to fit the data).

Fig. 3. Plot of interfacial capacitance versus potential for the oxidation and reduction of the PPyNQSA thin film.

the oxidation and reduction trend intersect in the region of the formal potential (300 mV).

This trend suggests a disruption to the direct electron transfer kinetics observed during oxidation. Evidence from SNIFTIRS suggests degradation of surface bound polymer units by anions in solution (e.g., Cl^-) which results in ring opening of surface polymer units and eventual loss of CO_2, similar to the structural degradation induced in pyrrole under strongly basic conditions [26]. This surface chemistry could explain the observed changes in EIS data and confirms the quasireversible oxidation kinetics predicted by the scan-rate-dependent CV. The difference between the complex plane impedance plots at 50 mV before oxidation and after reduction (Fig. 2) is further evidence of this.

3.3. SNIFTIRS

A shift of the baseline was evident in the spectra obtained at potentials increasingly positive of 0mV, when the spectra were viewed over the extended scale, covering the complete wavenumber range experimentally available, i.e., 5000 cm^{-1} to 1000 cm^{-1} (Fig. 4). This is related to low energy transitions within the polymer and is evidence of the conductive nature of the modified polymer. The solvent features seen at around 3500 cm^{-1} were not expected to interfere with other absorptions. During the analysis of spectral data however emphasis was placed on the absorptions between 1700 cm^{-1} to 1000 cm^{-1}, known as the fingerprint region of the spectrum. The intensity of absorption bands present in this region is indicative of the oxidation state of the polymer.

The bands present in the region of ring stretching are particularly intense due to strong coupling between charge carriers and ring vibrational modes, facilitating movement of carriers within conjugated polymer chains. These enhanced signals (IRAV bands) are typical of doped conducting polymers. The vibrations occur as paired bands at very close frequencies. The downward bands at 1531 and 1586 cm^{-1} were assigned to C=C and C−C vibrations. The bands at 1432 and 1380 cm^{-1} are assigned to C=N vibration. The band at 1294 cm^{-1} was assigned to N−H in plane contributions. Evidence of the sulfonic acid presence in the doped polymer was provided by the absorption bands at 1172 and 1080 cm^{-1}, assigned to the asymmetric stretch of the O=S=O group (Fig. 5) [36–39].

An absorption band at 2340 cm^{-1} which increased in intensity at potentials above 300 mV, is indicative of the presence of CO_2 [39–40].

3.4. Polymer Structure and Proposed Mechanism

During the first cycle of electrochemical polymerization of pyrrole an inner layer is formed upon which the polymerized polypyrrole grows. Subsequent cycling steps allow for the development of the polymer chain resulting in the main layer and the thickness thereof depends on the number of potential cycles employed. It is also the main layer that
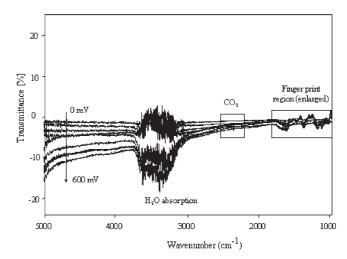

Fig. 4. Full SNIFTIRS spectra of PPyNQSA at 100 mV potential intervals from 0 to 600 mV, vs. calomel electrode.
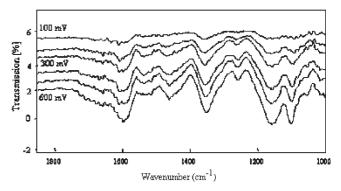

Fig. 5. Normalized SNIFTIRS spectra of PPyNQSA showing the enlargement of the finger print region.

influences overall film stability. The outer layer is produced by polymer termination when the potential is turned off and is made up of mainly short chain polypyrrole and therefore less stable than the main layer (Fig. 6a). When the polypyrrole film is oxidized at 315 mV (vs. Ag/AgCl) the surfactant anions (A^-) align close to the polymer surface to compensate for the positive charge caused by the formation of bipolarons under anodic potentials (Fig. 6b). This phenomenon is sometimes referred to as electroneutrality coupling and results in electron hopping within the polymer main layer to accommodate the bipolaron/ anion coupling at the surface [41].

While actuating the polymer in monomer free 0.05 M HCl, the entrapped 1, 2-napthaquinone-4-sulfonate (NQS^-) anion is immobile, it does not move and ionic transport is strictly determined by the hydrated small proton. However, with prolonged actuation or overoxidation, there is breakdown of the surface bound pyrrole and sulfonated units. The surfactant anion, NQS^{-1}, which is formed upon dissociation in the electrolyte behaves as a weak base. The surface bound pyrrole units loose the protons on the nitrogen in order for the surfactant to return to the preferred acidic state. The loss of the proton on the
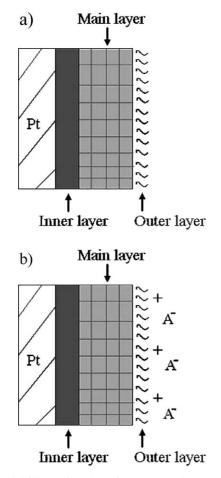
Fig. 6. Model illustrating the alignment of charges at different oxidation states of polypyrrole: a) neutral polymer and b) oxidized polymer.

pyrrole rings however leads to disruption of the cyclic structure by rearrangement to form hydroxyl and carbonyl species and eventual loss of material through formation of CO_2 [39].

This suggests that some pyrrole units on the surface of modified polypyrrole chain undergoes ring opening [26]. The lone pair on the ring nitrogen combined with the four π electrons of the two double bonds to give pyrrole an aromatic sextet of electrons. The nitrogen is sp^2-hybridised and acquires a positive charge as its lone pair is delocalized around the ring [42, 43]. Therefore we propose a mechanism for the oxidation of the polymer, which involves adsorption of the surfactant onto the polypyrrole film on the electrode surface. The interaction of the surfactant anion with the strongly polarized surface pyrrole units on the polymer backbone leads to disruption of the induced aromaticity on the pyrrole. This results in the protonation of the surfactant to yield the sulfonic acid and deprotonation of the ring nitrogen. Further overoxidation in the acid medium favors the reduction of the double bond adjacent to the nitrogen, which leads to ring opening and subsequent rearrangement to produce the more stable imine structure. The oxidation is irreversible and subsequent electronic rearrangement trans-

forms slowly to yield the capacitive material observed under reduction conditions at around 200 mV vs. Ag/AgCl.

4. Conclusions

1, 2-Napthaquinone-4-sulfonate have been successfully incorporated into the matrix of polypyrrole on a platinum disc electrode through potential cycling in aqueous solution of pyrrole-monomer (0.1 M) and the sodium salt of 1, 2-napthaquinone-4-sulfonic acid-dopant (0.01 M) in 0.05 M HCl. The resulting polymer showed high conductivity, optical changes, spectroscopic transitions and good electro-activity. The high frequency response of the modified polymer could not display a complete semicircle expected for in the complex impedance plot due to the limitation of the instrument that can not accumulate impedance data above 100 kHz. However the low frequency response shows a gradual transition of the volumetric capacitance with potential under oxidative potential stepping, whereas the reductive stepping gave an irreversible trend as the polymer do not revert to the low frequency impedance during the oxidative stepping. There was good correlation of data between the electrochemical and spectroelectrochemical investigation on the modified polymer using cyclic voltammetry, differential pulse voltammetry, square wave voltammetry, electrochemical impedance spectroscopy and SNIF-TIRS. There was smooth transition from the neutral to the polaronic and bipolaronic states as it is switched through a potential window of − 400 through 700 mV vs. Ag/AgCl. It is worth noting that the NQSA doped polypyrrole showed strong emissions in aqueous dispersion, which provides indication of potential applications in fabrication of various optometric devices. The application of this modified poly-pyrrole for biosensors and chemosensors is being investigated.

6. References

[1] L. Qu, G. Shi, J. Yuan, G. Han, F. Chen, *J. Electroanal. Chem.* **2004**, *561*, 149.
[2] J. Bobacka, *Electroanalysis* **2005**, *18*, 7.
[3] R. O. Akinyeye, M. Sekota, P. Baker, E. Iwuoha, *Fullerenes, Nanotubes and Carbon Nanostructures* **2006**, *14*, 49.
[4] Y. Yang, J. Liu; M. Wan, *Nanotechnology* **2002**, *13*, 771.
[5] A. Kassim, Z. B. Basar, H. N. M. E. Mahmud, *Proc. Indian Acad. Sci (Chem. Sci.)* **2002**, *114*, 155.

[6] Z. Wei, Z. Zhang, M. Wan, *Langmuir* **2002**, *18*, 917.
[7] J. Y. Lee, D. Y. Kim, C. Y. Kim, *Synth. Met.* **1995**, *74*, 103.
[8] R. Turcu, R. Grecu, M. Brie, I. Peter, A. Bot, W. Graupner, *Studia universitatis babes-bolyai, Physica, special issue* **2001**, 216.
[9] S. Asavapiriyanont, G. K. Chandler, G. A. Gunawardena, *J. Electroanal. Chem.* **1984**, *177*, 229.
[10] H. Masunda, D. K. Asano, *Synth. Met.* **2003**, *135 – 136*, 43.
[11] F. Cheng, M. Zhang, H. Wang, *Sensors* **2005**, *5*, 245.
[12] H. Shiigi, M. Kishimoto, H. Yakabe, B. Deore, T. Nagooka, *Anal. Sci.* **2002**, *18*, 41.
[13] Y. Lu, A. Pich, H. Adler, *Synth. Met.* **2003**, *135 – 136*, 37.
[14] T. K. Vishnuvardhan, V. R. Kulkarni, C. Basavaraja, S. C. Raghavendra, *Bull. Mater. Sci.* **2006**, *29*, 77.
[15] M.-A. Paoli A. Zanelli, M. Mastragostino, A. M. Rocco, *J. Electroanal. Chem.* **1997**, *435*, 217.
[16] D. Han, H. J. Lee, S. Park *Electrochim. Acta* **2004**, *50*, 3085.
[17] J. Wang, *Chem. Eur. J.* **1999**, *5*, 1681.
[18] J. Wang, M. Jiang, *Langmuir* **2000**, *16*, 2269.
[19] A. Ravanaviciene, A. Ravanavicius, *Anal. Bioanal. Chem.* **2004**, *379*, 287.
[20] B. D. Malhorta, A. Chaubey, S. P. Singh, *Anal. Chim. Acta*, doi: 10.1016/j.aca.**2006**.04.055.
[21] A. Ramanavičious, A. Ramanavičienė, A. Malinaukas, *Electrochim. Acta* **2006**, in press.
[22] A. A. Yakovleva, *Rus. J. Electrochem.* **2000**, *36*, 1275.
[23] J. Stejskal, M. Omastová, S. Fedorova, J. Prokeš, M. Trchová, *Polymer* **2003**, *44*, 1353.
[24] A. S. Viana, L. M. Abrantes, G. Jin, S. Floate, R. J. Nicholas, M. Kalaji, *PhysChemChemPhys* **2001**, *3*, 3411.
[25] Y. Martínez, R. Hernandez, M. Kalaji, O. P. Márquez, J. Márquez. *J. Electroanal. Chem.* **2004**, *563*, 145.
[26] H. Xie, M. Yan, Z Jiang, *Electrochim. Acta* **1997**, *42*, 2361.
[27] E. Smela, *J. Micromech. Microeng.* **1999**, *9*, 1.
[28] A. P. Brown, F. C. *Anson, Anal. Chem.* **1977**, *49*, 1589.
[29] A. J. Bard, L. R. Faulkner, *Electrochemical Methods – Fundamentals and Applications*, 2nd ed., Wiley, New York **2001**, pp. 239 – 256.
[30] R. S. Nicholson, *Anal. Chem.* **1965**, *37*, 1351.
[31] P. Zanello, *Inorganic Electrochemistry (Theory, Practice and Applications)*, Royal Society of Chemistry, Cambridge, UK, **2003**, pp. 49 – 135.
[32] R. Pauliukaite, C. M. A. Brett, A. P. Monkman, *Electrochim. Acta* **2004**, *50*, 159.
[33] F. Sundfors, J. Bobacka, A. Ivaska, A. Lewenstam, *Electrochim. Acta* **2002**, *47*, 2245.
[34] M. Grzeszczuk, G. Żabińska-Olszak, *J. Electroanal. Chem.* **1997**, *427*, 169.
[35] P. J. Mahon, G. L. Paul, S. M. Keshishian, A. M. Vassallo, *J. Power Sources* **2000**, *91*, 68.
[36] A. Benyoucef, F. Huerta, J. L. Vázquez, E. Morallon, *Europ. Polymer J.* **2005**, *41*, 843.
[37] R. T. S. M. Lakshmi, M. K. Vyas, A. S. Brar, I. K. Varma, *Europ. Polymer J.* **2006**, *42*, 1423.
[38] A. K. Cuentas-Gallegos, P. Gomez-Romero, *J. New Mater. Electrochem. Systems* **2005**, *8*, 181.
[39] I. Rodríguez, B. R. Scharifker, J Mostany, *J. Electroanal.-Chem.* **2000**, *491*, 117.
[40] D. J. Fermín, H. Teruel, B. R. Scharifker, *J. Electroanal. Chem.* **1996**, *401*, 207.
[41] Y. J. Yuan, S. B. Aduloju, G. G. Wallace, *Europ. Polymer J.* **1998**, *35*, 1761.
[42] R. T. Morrison, R. N Boyd, *Organic Chemistry*, 15th ed., Allyn and Bacon, New York University, USA **1980**, pp. 1002 – 1026.
[43] G. M. Loudon, *Organic Chemistry*, Benjamin/Cummins, California, USA **1988**, pp. 1043 – 1090.